Defect annealing and the formation of Li-rich clusters in Al-Li alloys

1995 J. Phys.: Condens. Matter 7 4573

(http://iopscience.iop.org/0953-8984/7/23/026)

J. Phys.: Condens. Matter 7 (1995) 4573–4581. Printed in the UK

Defect annealing and the formation of Li-rich clusters in Al–Li alloys

H M Fretwell†, J A Duffy†, M A Alam†, H P Leighly Jr†‡ and J Walmsley§

† H H Wills Physics Laboratory, University of Bristol, Tyndall Avenue, Bristol BS8 1TL, UK

‡ Department of Metallurgical Engineering, University of Missouri–Rolla, Rolla, MO 65401, USA

§ Berkeley Technology Centre, Nuclear Electric plc, Berkeley, Gloucestershire GL13 9PB, UK

Received 9 January 1995, in final form 5 April 1995

Abstract. Positron annihilation lineshape measurements are conducted on pure Al, Al–1.9 at.% Li and Al–(12.0–12.5) at.% Li alloys. The recovery of each sample following quench and/or cold-work treatments is discussed in terms of vacancy migration and clustering, dislocation annealing and precipitation. The results indicate precipitation in both alloy concentrations but no positron trapping at dislocations. All cold-worked alloys show large vacancy clustering effects, providing strong evidence of vacancy agglomeration at precipitates.

1. Introduction

The need to produce lighter and stronger materials for aircraft manufacture has led to a considerable amount of interest in Al–Li-based alloys [1]. The Al-rich side of the Al–Li phase diagram [2, 3], consists of a simple eutectic between the FCC α solid solution and the BCC δ(AlLi) equilibrium phase. Quenching gives rise to a fine dispersal of coherent metastable $\delta'(Al_3Li)$ precipitates that inhibit dislocation movement and improve the strength of the alloy [4]. $\delta'(Al_3Li)$ precipitates are ordered [5] and almost perfectly coherent with the surrounding solid solution matrix. A low interfacial energy at the α/δ' boundary ensures that the precipitates are spherical over a large size range (2–300 nm) [6]. Most measurements reported in the literature so far have concentrated on room-temperature, water-quenched samples, where nucleation and growth of δ' are thought to be completed prior to ageing [7]. Small-angle neutron scattering [8] and TEM [9] experiments find that δ' coarsens according to Ostwald ripening kinetics. Large ($\leqslant$500 nm) dendritic δ' may form if the alloy is aged near the δ'/δ solvus line [6]. Prolonged ageing below the δ' solvus also heterogeneously precipitates the equilibrium δ(AlLi) phase at high-energy sites e.g. grain boundaries [7] and on highly strained δ'/matrix interfaces [10].

To exploit fully the strengthening properties and minimize the undesirable poor ductility of this alloy, it is important to understand the nucleation, growth, coarsening and dissolution of δ' precipitates and the role of vacancies and dislocations in these stages. It is hoped that the sensitivity of positrons to a range of defects, especially open volume defects, will provide additional information not obtainable by conventional techniques such as TEM. The aim of this paper is to build on previous positron annihilation work [11, 12, 13, 14] and to assess the role this technique can play, in conjunction with TEM, in studying the precipitation process. The feasibility of positron trapping at coherent precipitates, such as δ', depends

0953-8984/95/234573+09$19.50

upon the relative positron affinity of the alloy elements and the size, composition and number density of precipitates. The possibility of positrons trapping in Li-rich precipitates is good because of the large theoretical positron affinity differences between pure Al and Li metal [15]. Positrons find lithium one of the most attractive metals in existence. Therefore Li-rich precipitates of reasonable size and concentration should trap positrons. If positrons do become trapped in lithium-rich environments this will be reflected in the annihilation characteristics as a high S parameter (see later) value compared to pure annealed Al.

2. Experimental details

Two alloy concentrations, Al–1.9 at.% Li and Al–(12.0–12.5) at.% Li, were studied. Two batches of the high-Li-content alloys were combined to increase the total number of samples available. A difference of 0.5 at.% Li is unlikely to have an appreciable impact on the measurements at these high concentrations. The alloys were produced by melting high-purity (99.999%) materials, to which small quantities of zirconium (~0.06 at.%) were added. The inclusion of a small amount of zirconium inhibits recrystallization and leads to better control of the grain size [16]. A fine dispersal of coherent, metastable Al_3Zr precipitates forms during processing, which eventually form composite δ' with a central Al_3Zr core and an Al_3Li halo [17]. Zirconium has a weaker affinity than lithium and is marginally less attractive than aluminium [15]. Moreover the Zr-based precipitation is very finely dispersed suggesting Al_3Zr will be a small fraction of the composite δ' particles. Zr also has a lifetime of 163 ps [18] which is very close to the Al lifetime value of 165 ps [19]. For these reasons we envisage that the zirconium will not significantly affect positron trapping rates or the resulting annihilation characteristics, although it may have a small impact on the alloy annealing behaviour [12].

The precipitation and associated vacancy migration phenomena were investigated following quenching and/or low-temperature deformation of the specimens, designed to create specific non-equilibrium conditions. The samples were held at a homogenizing (solid solution) temperature of ~848 K for 15–20 minutes in a temperature-controlled (±2 K), argon atmosphere furnace, before quenching into a cold (200 K) bath of concentrated hydrochloric acid. The samples were then promptly transferred to liquid nitrogen for storage. A fuller description of the quenching furnace, procedure, cleaning and transfer procedures are given elsewhere [20]. Cold working was achieved by a hydraulic press with the sample immersed in liquid nitrogen to help induce defects below the vacancy migration temperature (vacancy migration in Al occurs at ~190 K [21]). The amount of deformation inflicted is measured by the percentage thickness reduction, $(D_i - D_f)/D_i$, where D_i and D_f are the initial and final sample thicknesses, respectively. Details of specimen treatment prior to annealing are given in table 1.

During each quench, a lithium depletion layer up to several hundred μm thick forms beneath the surface [22] which is comparable with the positron penetration depth (~0.1 mm in Al). After quenching the topmost ~0.3 mm of the surface is removed by polishing with fine grit abrasive under liquid nitrogen. The recovery of each heat-treated sample is monitored via the positron–electron line shape parameter S [19]. S is derived from the annihilation energy spectrum and is defined here as the central (±0.9 keV) of the Doppler-broadened 511 keV energy line normalized by the total counts in the peak. S reflects changes in the energy distribution due to changes in the environment at the annihilation site. In general, the annihilation of a trapped positron from a defect, e.g. dislocation, vacancy or a vacancy cluster, will lead to a narrower energy distribution and to a higher S parameter value compared to the bulk. We expect to see the following trends:

Table 1. Quench and cold-working procedures performed on Al–Li and Al samples.

Material	Heat treatment
Pure Al	Quenched (848–200 K).
Pure Al	Annealed at 793 K for 2 h, cooled slowly, cold-worked (23%).
Al–1.9 at.% Li	Quenched (848–200 K), surface removed at 77 K.
Al–1.9 at.% Li	Annealed at 793 K for 2 h, cooled slowly, cold-worked (23%).
Al–(12.0–12.5) at.% Li	Quenched (848–200 K), surface removed at 77 K.
Al–(12.0–12.5) at.% Li	Direct quench (i.e. cooled slowly from 848 to 573 K), aged at 573 K for 2–3 h, quenched to 300 K and surface removed, cold-worked (17.5%).
Al–12.0 at.% Li	Quenched (848–200 K), surface removed at 77 K, cold-worked (29%).

$S_{Al} < S_{Al-dislocation} < S_{Al-vac} < S_{Al-vacancy\ cluster}$ and $S_{Al} < S_{Li}$. When a positron annihilates from a combination of such states, the observed value will be a weighted average of the S_i values. Each energy spectrum is collected over a period of 30 minutes and contains 2–4 million counts. Simultaneously, the sample temperature is increased at ~10 K h^{-1}(±2 K) so that each point in a recovery curve corresponds to 5 degrees change in temperature. Experiments are pursued to high temperatures (670 K) and then cooled at a faster rate of –20 or –30 K h^{-1}, during which $S(T)$ is monitored.

3. Results and discussion

To assist in our interpretation of the positron annihilation results for the alloy samples, the recovery of pure Al was also studied. The S values are normalized such that $S(T)$ for a fully annealed Al specimen is equal to unity at 300 K. The alloy data have been renormalized with respect to annealed Al, by measuring $S(T)$ (with the same positron source) for each sample studied, following its anneal up to 670 K during the experiment. Thus the S values are normalized such that absolute values in figures 1–4 are directly comparable. Solid lines have been drawn through the data points to help guide the eye.

3.1. Recovery behaviour of pure aluminum

The recovery of quenched and cold-worked pure Al is shown in figure 1. In the as-quenched sample the majority of defects will be vacancies and possibly some small vacancy agglomerates. These vacancies begin migrating at ~190 K and form vacancy clusters that steadily grow until they can no longer sustain their volume and collapse into sessile dislocation loops (at 240 K) and the S parameter drops. The dislocation loops provide additional sinks for the remaining vacancies. The next sharp stage occurs at 400 K and is generally attributed to dislocation loop annealing. The exponential rise in S at higher temperatures reflects the increasing thermal vacancy population [23].

Cold-worked aluminium has a more complex recovery given the wider range of defects present. In the as-cold-worked state the defects include dislocations, vacancies, vacancy clusters, and possibly interstitial clusters and the high initial S parameter is a reflection of this. There is very little change until 190 K when the S parameter drops sharply to be followed by a small peak at ~260 K. Similar features have been seen in the literature and have been attributed to the divacancy and monovacancy annealing stages [13]. An alternative explanation may involve vacancy migration at 190 K with immediate loss to sinks (dislocations) followed by remnant clustering at stable nucleation centres, generating the second peak (260 K). Above 260 K there are several broad stages whose precise origins

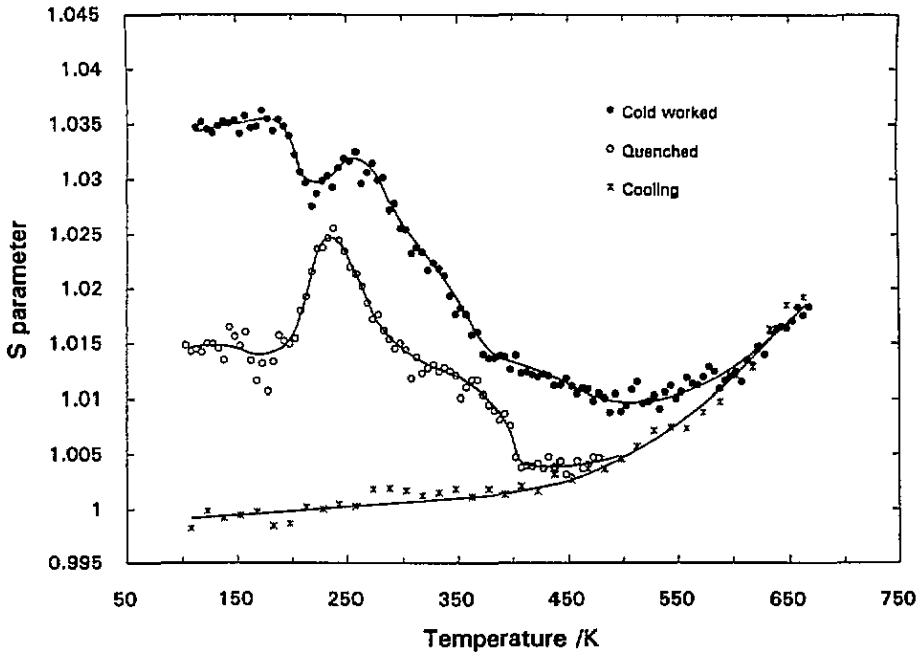

Figure 1. Positron lineshape parameter S as a function of annealing temperature for quenched and cold-worked (23%) aluminium.

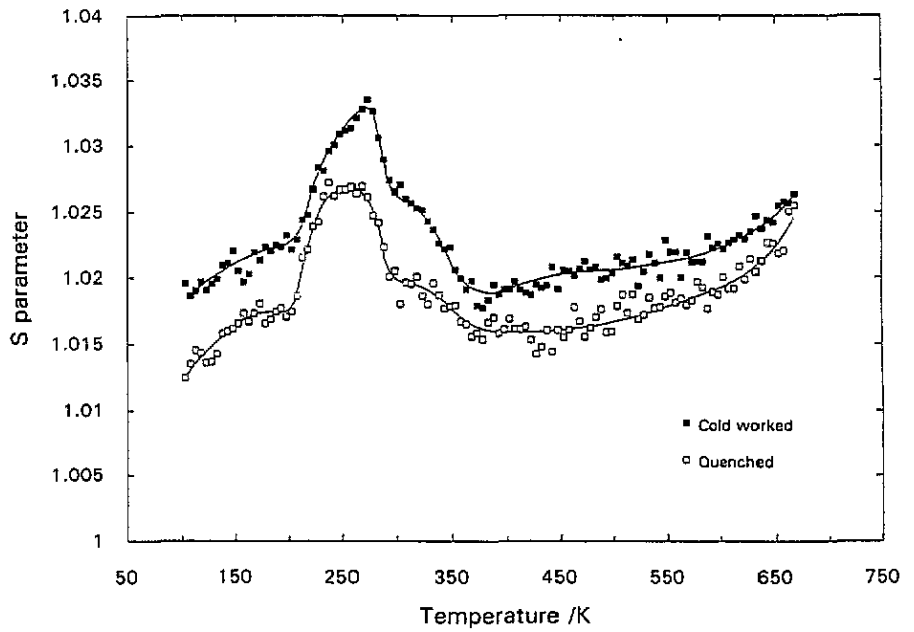

Figure 2. Positron lineshape parameter S as a function of annealing temperature for quenched and cold-worked (23%) Al–1.9 at.% Li.

are unclear, but may stem from the annealing of the remnant vacancy clusters, combined with the loss of dislocations during recrystallization.

3.2. Recovery behaviour of Al–1.9 at.% Li

By adding a small amount of lithium to the sample the recovery scenario is radically altered (figure 2). The inclusion of lithium may affect the generation of defects, as well as increasing the range of positron traps available in the form of precipitates, precipitate/defect and Li/defect complexes. From the phase diagram [3] one would expect to quench in a saturated solid solution and no δ' phase, although there is a possibility of δ(AlLi) precipitation given the wide uncertainty in the α/δ solvus position [2]. Annealing of the quenched sample reveals a distinct peak in S at ~250 K, similar to that found in pure quenched aluminium (at ~240 K), although broader and at a slightly higher temperature than in Al. It seems plausible that we are again observing micro-void growth and collapse, but moderated by Li–vacancy binding, whose effect is to retard the process by either stabilizing the microvoids or slowing their growth rate. Residual traps exist between 290 and 375 K and the sharp dislocation loop annealing stage observed in quenched aluminium at 400 K is no longer seen. If Li-rich precipitates are responsible for trapping some positrons, as suggested by the overall higher S values above 290 K, then dislocation loop defects, if present, may not be seen above these new competitive traps.

The recovery for the same (Al–1.9 at.% Li) alloy after cold working at 77 K differs little from the quenched sample (figure 2). Despite the high density of vacancy sinks in the sample, i.e. deformation-induced dislocations, a strong vacancy clustering peak is again observed (at ~260 K); providing further confirmation of vacancy–impurity binding effects, similar to those found in cold-worked Ni alloys [24]. Surprisingly, there is little evidence for positron dislocation trapping or a dislocation annealing stage at higher temperatures. The annealing curve for the deformed sample closely resembles the quenched one above 375 K and lies only slightly above the equilibrium cooling curve (not shown), but not high enough to suggest significant trapping at dislocations. Our own TEM (transmission electron microscopy) work on this low-concentration alloy (cold worked and heated steadily to 480 K) showed some evidence of small (<10 nm) precipitates. It appears that dislocations are not as strong positron traps as these precipitates. The post-annealing cooling curve for both quenched and cold-worked samples (not shown) lie significantly above that for annealed Al, a further indication of significant positron trapping at Li-rich precipitates that remain in the sample even after heating to 670 K.

It is not possible to identify the type or composition of the precipitates from the positron data in the presence of so many competing positron traps. We can only infer their existence from the impact on the vacancy clustering process and the indication of a new type of positron trap above 375 K that masks all dislocation annealing behaviour. From the phase diagram we suppose the type of precipitate responsible in the low-concentration alloy will be δ(AlLi) or perhaps Zr based and further TEM work is proposed here.

3.3. Recovery behaviour of Al–(12–12.5) at.% Li

The recovery of the quenched high-Li-content sample is presented in figure 3 together with those for pure Al and Al–1.9 at.% Li for comparison. In the high-concentration alloy, recovery is complicated by the inevitable presence of δ' precipitates [7]. The initial level of S is high, compared with either quenched or deformed Al, suggesting the creation of Li-rich positron trapping environments in the as-quenched state. In light of the fact that water-quenched samples contain a high number of δ' particles immediately after quenching [7], it reasonable to assume that the positron traps indicated here are also δ' or are precursors to δ'.

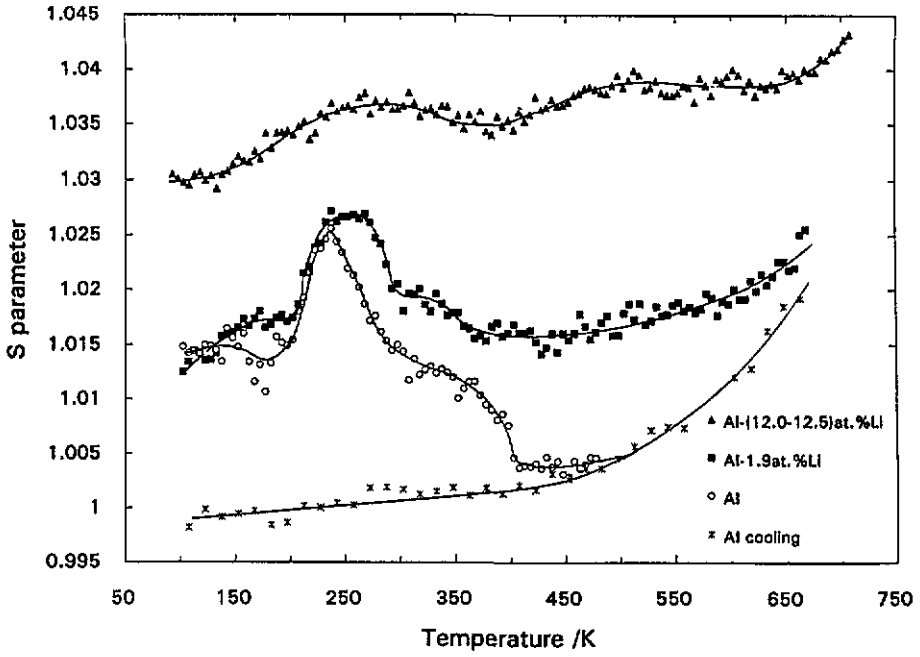

Figure 3. Positron lineshape parameter S as a function of annealing temperature for quenched Al, Al–1.9 at.% Li and Al–(12.0–12.5) at.% Li.

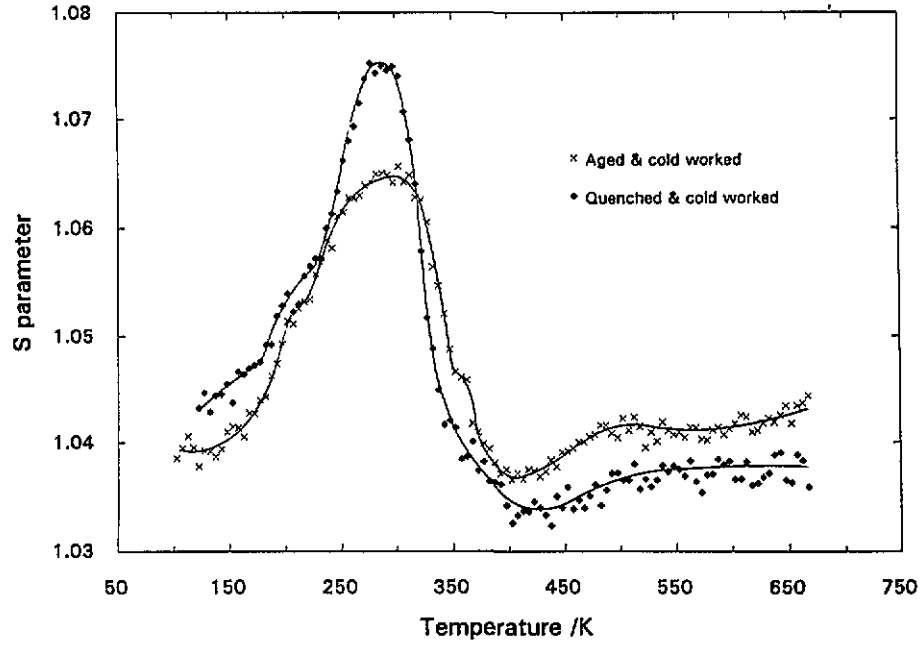

Figure 4. Positron lineshape parameter S as a function of annealing temperature for Al–(12.0–12.5) at.% Li, (i) aged then cold-worked (17%) (see text) (ii) quenched then cold-worked (29%).

As the temperature is increased a very shallow, broad peak (centred at 280 K) is observed. A possible explanation for such a weak feature (compared to the low-

concentration alloy) may lie in a low concentration of quench-induced vacancies. The comparatively high concentration of mobile Li atoms at high temperatures prevailing during the initial stages of the quench may facilitate a rapid migration of vacancies to sinks during cooling. In this scenario the remaining vacancies in the as-quenched state are bound to Li (atoms and/or precipitates) resulting in the retarded, broad vacancy clustering peak.

Further evidence for a low concentration of quenched in vacancies is found if a quenched specimen is immediately cold worked. There a significant vacancy clustering effect is observed in the form of an abnormally large peak at 300 K (figure 4). Cold working introduces free vacancies which can migrate above 190 K. If they cluster at Li-rich precipitates the S parameter will reflect vacancies, vacancy clusters and lithium resulting in a very high value, as observed. If the vacancies then dissociate from the precipitates the changes will be correspondingly large. It has also been pointed out to us that positronium formation at microvoids cannot be ruled out. In either case we suggest that the vacancy agglomerates must be associated with the Li-rich precipitates in such a highly deformed material.

To investigate the effect of introducing an excess vacancy concentration on existing large δ' precipitates, a sample was aged at 573 K for 2–3 h to produce large dendritic δ' particles, quenched to room temperature and cold worked. Again a huge peak is seen at 300 K (figure 4), similar to that seen in other work [13]. The similarity of the two peaks at 300 K indicates that the underlying processes are largely independent of the initial precipitate size. Although some kind of vacancy migration and clustering must be associated with this peak, it is unlikely that such large changes in S (6.5% and 7.5% above annealed Al at 300 K) are due solely to vacancy clustering and are more likely to due to a reorganization of Li-rich precipitates (probably δ'), mediated by the migration and/or clustering of deformation-induced vacancies. The magnitude of the 300 K peak in the aged sample is slightly smaller, in line with the smaller degree of deformation and concentration of vacancies.

Finally, all high-concentration quenched and cold-worked samples show similar high-temperature (~400–670 K) behaviour, irrespective of the dislocation density and prior heat treatments. Dislocations, thermal vacancies, δ and δ' precipitates are the only possible positron traps at these higher temperatures (dislocations are observed in cold-worked Al up to ~550 K). The similarities between the quenched and cold-worked samples above 400 K are a good indication that the positron is insensitive to dislocations due to competitive trapping at δ' precipitates, as suggested by de Diego *et al* [14]. δ' is likely to be the predominant positron trapping precipitate, given its much higher number density and homogeneous distribution compared with δ. Further evidence for positron trapping at δ' is suggested by the convergence of the annealing and cooling curves (not shown) at a temperature of ~620–630 K close to the expected dissolution of δ' at 600 K [3]. This convergence occurs for all high-concentration alloy annealing curves and is independent of the initial heat treatment of the sample.

At 670 K the S parameter for Al–(12.0–12.5) at.% Li ($S \sim 1.04$) remains high and does not approach the pure Al ($S \sim 1.02$) or Al–1.9 at.% Li ($S \sim 1.025$) level, thus suggesting residual positron trapping at substantial Li-rich clusters such as δ. A similar discrepancy is seen on cooling (not shown), with the high-concentration alloy lying well above both the low-concentration alloy and pure Al. Slow cooling of the high-lithium-content alloy is likely to favour the growth of the δ phase unlike the metastable δ' which is formed on rapid quenching and the higher levels of S in comparison with the low-concentration alloy may reflect a higher density of δ precipitates.

Again, it is difficult to verify the types of Li-rich precipitate responsible for the positron trapping behaviour from the lineshape parameter alone. The data are consistent with trapping

at Li-rich regions and we infer that both δ' and δ give rise to positron trapping in the high-concentration alloy.

4. Summary

The positron annihilation work does offer some interesting observations.

(i) A high initial S parameter in the quenched high-concentration alloy suggests that Li-rich environments are formed immediately on quenching below room temperature. These are possibly δ' or precursors to the δ' phase.

(ii) Vacancy clustering is 'retarded' in quenched Al–Li alloys as the Li concentration is increased.

(iii) The results suggest that fewer vacancies are retained on quenching the high-concentration alloy compared with the low-concentration one.

(iv) Vacancy clustering effects are observed in all cold-worked alloy samples, despite a high density of vacancy sinks. In high-Li-concentration alloys these effects are highly pronounced suggesting the clustering is associated with Li-rich precipitates (possibly δ').

(v) Preferential positron trapping at Li-rich precipitates is suggested to account for the lack of dislocation or dislocation loop annealing stages in highly deformed and quenched alloy samples.

(vi) The formation of Li-rich precipitates is inferred from both positron and TEM experiments in low-concentration alloys where such entities are not expected in equilibrium in the binary alloy.

Further TEM work is under way to complement the positron annihilation data discussed.

Acknowledgments

The authors would like to thank Keith Dinsdale (University of Nottingham) for the specimens, Stephen Usmar and Maurizio Biasini for valuable suggestions and Richard Head and Ken Dunn and staff for technical assistance. This work was supported by grants from the EPSRC, UK and the Royal Commission for the Exhibition of 1851.

References

[1] Martin J W 1988 *Ann. Rev. Mater. Sci.* **18** 101
[2] Fujikawa S, Izeki Y and Hirano K 1986 *Scr. Metall.* **20** 1275
[3] Williams D B 1989 *Aluminium–Lithium Alloys V: Proc. 5th Int. Conf. (Williamsburg, VA, 1989)* ed T H Sanders Jr and E A Starke Jr (Birmingham: Materials and Component Engineering) p 551
[4] Lavernia E J, Srivatsan T S and Mohamed F A 1990 *J. Mater. Sci.* **25** 1137
[5] Sato T, Tanaka N and Takahaski T 1988 *Trans. Japan Inst. Met.* **29** 17
[6] Chabala J M, Levi-Setti R, Soni K K and Williams D 1991 *Appl. Surf. Sci.* **51** 185
[7] Bauman S F and Williams D B 1985 *Metall. Trans. A* **16** 1203
[8] Abis S, Caciuffo C, Carsughi F, Coppola R, Magnani M, Rustichelli F and Stefanon M 1990 *Phys. Rev.* B **42** 2275
[9] Mahalingam K, Gu B P, Liedl G L and Sanders T H Jr 1987 *Acta Metall.* **35** 483
[10] Samuel F H and Champier G 1987 *J. Mater. Sci.* **22** 3851.
[11] Dlubek G, Krause H, Krause S and Lademann P 1992 *Positron Annihilation: Proc. 9th Int. Conf. on Positron Annihilation (Szombathely, Hungary, 1991)* ed Z Kajcsos and C Szeles (Switzerland: Trans Tech) p 977
[12] Dlubek G, Krause S, Krause H, Welpmann K and Peters M 1992 *Scr. Metall.* **27** 1049
[13] de Deigo N, Segers D, del Rio J, Dorikens-Vanpraet L and Dorikens M 1991 *J. Phys.: Condens. Matter* **3** 5415

[14] de Diego N, del Rio J, Segers D, Dorikens-Vanpraet L and Dorikens M 1993 *Phys. Rev.* B **48** 6781
[15] Puska M J, Lanki P and Nieminen R M 1989 *J. Phys.: Condens. Matter* **1** 6081
[16] Gu B P, Mahalingam K, Liedl G and Sanders T H Jr 1986 *Aluminium–Lithium Alloys III: Proc. 3rd Int. Aluminium-Lithium Conf. (Oxford, UK, 1986)* ed C Baker, P J Gregson, S J Harris and C J Peel (London: Institute of Metals) p 360
[17] Gayle F W and Vandersandle J B 1984 *Scr. Metall.* **18** 473
[18] Sharma S M, Sikka S K and Chidambaram R 1985 *Positron Annihilation: Proc. 7th Int. Conf. on Positron Annihilation (New Dehli, India, 1985)* ed P C Jain, R M Singru and K P Gopinathan (Singapore: World Scientific) p 52
[19] MacKenzie 1983 *Positron Solid-State Physics: Proc. Int. School of Physics 'Enrico Fermi' (Varenna, Italy, 1981)* ed W Brandt and A Dupasquier (Amsterdam: North-Holland) p 196
[20] Alam M A and West R N 1982 *J. Phys. F: Met. Phys.* **12** 389
[21] Peterson K 1983 *Positron Solid-State Physics: Proc. Int. School of Physics 'Enrico Fermi' (Varenna, Italy, 1981)* ed W Brandt and A Dupasquier (Amsterdam: North-Holland) p 298
[22] Papazian J M, Schulte R L and Adler P N 1986 *Metall. Trans.* A **17** 635
[23] West R N 1979 *Positrons in Solids (Springer Topics in Current Physics 12)* ed P Hautojärvi (Berlin: Springer) p 89
[24] Dlubek G, Krause R, Brummer O, Michno Z and Gorecki T 1987 *J. Phys. F: Met. Phys.* **17** 1333